RESEARCH COMMUNICATION

Evaluation of the Geometric Accuracy of Anatomic Landmarks as Surrogates for Intrapulmonary Tumors in Image-guided Radiotherapy

Hong-Sheng Li[1,2], Ling-Ling Kong[2], Jian Zhang[1], Bao-Sheng Li[2]*, Jin-Hu Chen[3], Jian Zhu[3], Tong-Hai Liu[3], Yong Yin[3]

Abstract

Objectives: The purpose of this study was to evaluate the geometric accuracy of thoracic anatomic landmarks as target surrogates of intrapulmonary tumors for manual rigid registration during image-guided radiotherapy (IGRT). Methods: Kilovolt cone-beam computed tomography (CBCT) images acquired during IGRT for 29 lung cancer patients with 33 tumors, including 16 central and 17 peripheral lesions, were analyzed. We selected the "vertebrae," "carina," and "large bronchi" as the candidate surrogates for central targets, and the "vertebrae," "carina," and "ribs" as the candidate surrogates for peripheral lesions. Three to six pairs of small identifiable markers were noted in the tumors for the planning CT and Day 1 CBCT. The accuracy of the candidate surrogates was evaluated by comparing the distances of the corresponding markers after manual rigid matching based on the "tumor" and a particular surrogate. Differences between the surrogates were assessed using 1-way analysis of variance and post hoc least-significant-difference tests. Results: For central targets, the residual errors increased in the following ascending order: "tumor," "bronchi," "carina," and "vertebrae;" there was a significant difference between "tumor" and "vertebrae" ($p = 0.010$). For peripheral diseases, the residual errors increased in the following ascending order: "tumor," "rib," "vertebrae," and "carina;" There was a significant difference between "tumor" and "carina" ($p = 0.005$). Conclusions: The "bronchi" and "carina" are the optimal surrogates for central lung targets, while "rib" and "vertebrae" are the optimal surrogates for peripheral lung targets for manual matching of online and planned tumors.

Keywords: Cone-beam CT - image-guided radiotherapy - lung cancer - image registration - manual matching

Asian Pacific J Cancer Prev, **13**, 2393-2398

Introduction

A major advancement in radiotherapy in recent years is the advent of image-guided radiation therapy (IGRT). At present, there are a variety of clinically available IGRT technologies, including electronic portal imaging devices (EPIDs), kilovolt (kV) CT-on-rail, helical tomotherapy (megavolt, MV), and kV/MV cone-beam computed tomography (CBCT). The two-dimensional (2D) EPID is the simplest form and is conventionally employed to verify and correct positional uncertainties (Herman et al., 2001; Dirkx et al., 2006). An EPID with a well-thought-out correction protocol may be sufficient for some disease sites (e.g., the brain, head, and neck) where bony landmarks can be reliably used to determine the target and critical organ locations (Bel et al., 1995; de Boer et al., 2001). However, it produces poor soft-tissue contrast. Meanwhile, three-dimensional (3D) imaging devices, such as kV CBCT, can generate images with improved soft-tissue contrast by using acceptably low imaging doses. Thus, in comparison to EPIDs, IGRT by using 3D imaging may improve tumor targeting during the delivery of radiotherapy.

At present, it is permitted for a combination of computer-automated and manual registrations with 3D image-guided platform for radio-oncologists. However, there are different results between automatic and manual target matching are observed in clinical workflow (Guckenberger et al., 2006; Yeung et al., 2009). It is commonly accepted that automated registration should be followed by manual verification of the visible tumors to determine if the target position is consistent with the planning target volume (PTV). In cases where the target is outside the PTV, manual adjustments are made to avoid a mismatch (Thilmann et al., 2006; Bissonnette et al., 2009; Higgins et al., 2009; Chen et al., 2011), however, some confusion still exists in the practice of employing manual registration of the planning CT and online volumetric images of lung tumors. First, if the tumor is

*[1]Department of Radiation Oncology, Cancer Hospital and Institute, Tianjin Medical University, Tianjin, [2]Department of Radiation Oncology (Chest Section), [3]Department of Radiation Physics, Key Laboratory of Radiation Oncology of Shandong Province, Shandong Cancer Hospital and Institute, Jinan, China *For correspondence: pubmed@sohu.com*

round or oval and large, the tumors in adjacent slices will also be similar, making manual slice-to-slice matching very difficult. Second, tumor shrinkage and deformation are frequent observed in small-cell lung cancers or radiation-sensitive non-small-cell lung cancers by using 3D conformal radiotherapy, especially for synchronizing radio-chemotherapy. Therefore it is obviously difficult to manually match the deformed lung tumor to a planned one. Thus, systematic clinical studies are needed to compare different anatomic landmarks around lung tumors to identify the best surrogate of the target for manual matching. Such information will be helpful to resolve the aforementioned difficulties in 3D image-guided lung radiotherapy. In addition, when it is difficult to manually register tumors directly between online EPID images and planned ones, the matching of surrogates may be a better choice, potentially resulting in results similar to those with 3D IGRT.

In the clinical practice of image guidance, some radio-oncologists take bone tissues (e.g., vertebrae, ribs, etc.) as surrogates of the lung tumor (Wang et al., 2007; Song et al., 2007; Bissonnette et al., 2009) while others perform image-guided lung radiotherapy by matching soft tissues (e.g., tumor, carina, etc.) directly (Guckenberger et al., 2007; Purdie et al., 2007; Grills et al., 2008; Yeung et al., 2009; Boda-Heggemann et al., 2011). However, the optimal surrogate of lung tumors is unknown. In the present study, we investigated the geometric accuracy of several anatomic landmarks as surrogates of lung tumors for image-guided lung radiotherapy.

Materials and Methods

Patient population

From June 2009 to September 2011, 42 lung cancer patients with 48 intrapulmonary tumors (maximum of 2 lesions per patient) including 20 central tumors and 28 peripheral tumors treated with 3D conformal radiotherapy were recruited in the present retrospective study. Image guidance was performed using online kV CBCT (Varian OBI, Varian Medical Systems, Palo Alto, CA, USA) images for all the patients at least once a week.

Radiation simulation and planning

All the patients underwent radiation simulation with kV helical CT. Patients were immobilized with an individually molded whole-body vacuum cushion in the supine position. The conventionally used radiation simulation setup involves wall lasers aligned to 3 tattoos marked on the skin of the patient. The planned isocenter was determined on the basis of the system established by 3 external coordinates. All the patients had received free shallow breathing spiral CT scans (Brilliance Big Bore CT, Philips Medical Systems, Inc. Cleveland, OH, USA) for the neck and whole chest. The "rotation time" of the CT scanner's gantry was 1.0 s, and the reconstruction slice thickness was 3.0 mm.

After the planning CT images were transferred to the Eclipse Treatment Planning System (Varian Medical Systems, Palo Alto, CA, USA; version 8.5), the gross tumor volume (GTV) was delineated. Tumor motion was conventionally evaluated using a Varian Ximatron Simulator (Varian Medical Systems, Palo Alto, CA, USA) before the kV helical CT simulation, and a margin of 8-10 mm was applied to compensate for set-up error and target motion. After contouring the target volumes and organs at risk, a CRT plan was designed using a combination of 4-6 coplanar beams without couch angles. Depending on the tumor location, pathological type, and Tumor (T), Node (N), Metastasis (M) staging, different fractionation schemes were applied. Total doses ranged from 45 Gy to 74 Gy with 1.8 or 2.0 Gy per fraction.

CBCT image acquisition and online registration

Image guidance and treatment delivery were performed during free breathing by employing a linear accelerator (Trilogy, Varian Medical Systems, Palo Alto, CA, USA) equipped with an on-board kV CBCT. On the treatment day, following conventional initial setup with wall lasers aligned to the external skin tattoos made during the initial simulation, a CBCT volumetric image was acquired according to the standard protocol; approximately 650 projections were collected as the gantry rotated 360° counterclockwise, which took approximately 60 s. The kV exposure settings were as follows: 100 kV, 20 mA, and 20 ms per frame. The CBCT reconstruction slice thickness was 3.0 mm.

After image reconstruction, the CBCT image was automatically registered to the planning CT image by using a computer on the basis of the mutual information matching algorithm. If the results of registration by visual judgment were not ideal, the CBCT volume was immediately manually registered to the reference planning CT according to landmarks such as the bone and soft tissues around the target or distinctive anatomy in the target. This target position error was corrected by adjusting the patient position through shifting the treatment couch. The treatment commenced immediately after online setup verification and correction.

Retrospective offline registration

To exclude the impact of large interfractional deformation during the course of fractional radiotherapy, residual errors (REs) after manual registration were evaluated only between the first fraction dataset (Day 1 CBCT) and the planning CT. Three to six identifiable small markers (markers a, b, c, etc.; diameter, 1.0 mm) were

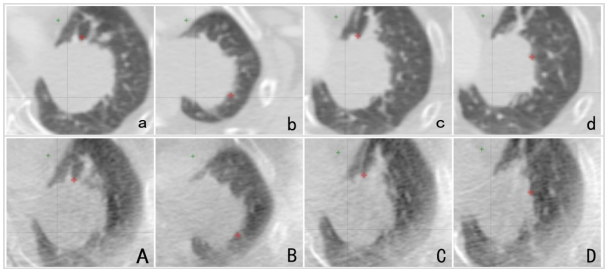

Figure 1. Corresponding Markers Noted in the Tumor of Planning CT and Day 1 Cone-beam Computed Tomography (CBCT) (a–d) Examples of markers (red points) noted in the tumor of planning CT; (A–D) the corresponding markers (red points) noted in the same tumor of CBCT in the axial plane

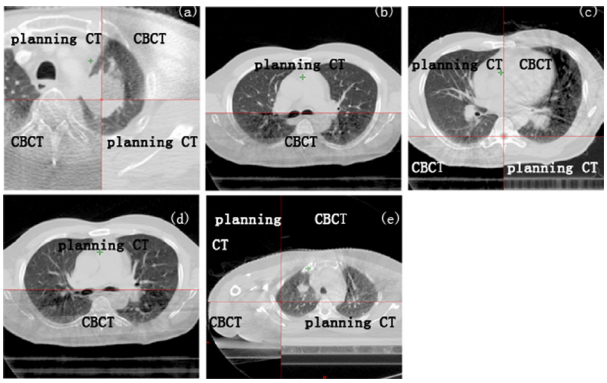

Figure 2. An Example of Successful Manual Rigid Registration of CBCT and Planning CT Images in the Axial Plane. The registrations of CBCT and planning CT images were based on "tumor" matching (a), "carina" matching (b), "vertebrae" matching (c), "large bronchi" matching (d), and "rib" matching (e)

noted offline in the tumor on the planning CT image. Day 1 CBCT was imported to the Eclipse Treatment Planning System, and the corresponding small markers (markers A, B, C, etc.; diameter, 1.0 mm) were subsequently noted in the tumor of the CBCT image. Figures 1a–d show an example of markers noted in the tumor of the planning CT. Meanwhile, Figures 1A–D show the corresponding markers noted in the tumor in CBCT in the axial plane. The planning CT and Day 1 CBCT datasets were retrospectively registered using different manual registration methods ("tumor," "thoracic vertebrae," "tracheal carina," and "large bronchi" for central diseases; "tumor," "thoracic vertebrae," "tracheal carina," and "rib" for peripheral lesions) in the axial, coronal, and sagittal planes until the target surrogates were perfectly matched by visual judgment. The 3D distances between corresponding markers (a–A, b–B, c–C, etc.) were measured separately for each dimension: left–right, superior–inferior, and anterior–posterior. Next, the 3D vectors of the corresponding markers were calculated according to the following equation: , where X, Y, and Z represent the left–right, superior–inferior, and anterior–posterior directions, respectively. A radiation oncologist with 2 therapists who were well trained in CBCT image-guided radiotherapy executed the offline registration procedure. Figure 2 shows an example of successful manual image registration in the procedure using "tumor," "tracheal carina," "thoracic vertebrae," "large bronchi," and "rib."

Evaluation of the surrogates for IGRT

The means of the 3D vectors between each pair of the corresponding markers of a particular surrogate were calculated to evaluate the discrepancy (i.e., the RE) between the positions of the planned and actual tumors one after manual registration. A smaller RE of a particular surrogate indicated that the target was matched better. Because the lung tumor itself is a target, a surrogate "tumor" was assumed to be the gold standard of manual registration. We evaluated the statistical differences between "tumor" and the other surrogates using 1-way analysis of variance (ANOVA) and post hoc least-significant-difference tests by using SPSS 10.0 for Windows (SPSS Inc., Chicago, IL, USA). If there was significant difference between "tumor" and a particular surrogate, the surrogate was rejected as a registration template. Two-tailed p-values < 0.05 were considered statistically significant.

Table 1. Clinical Characteristic of Patients

Tum. ID.	Location	Classification	Histologic type	Vol. (cm^3)	D_{max} (cm)
1	LML	Cent. D	SCC	6.89	2.81
2	LUL	Cent. D	SCC	63	4.65
3	LUL	Cent. D	SCC	58.13	4.7
4	LLL	Cent. D	SCLC	4.41	1.95
5	RML	Cent. D	SCC	87.27	8.43
6	LLL	Cent. D	Adeno.	25.15	5.5
7	RML	Cent. D	Adeno.	24.46	5.15
8	RML	Cent. D	SCC	16.4	3.4
9	RML	Cent. D	SCC	19.22	3.2
10	LUL	Cent. D	Adeno.	30.19	4.8
11	LLL	Cent. D	Adeno.	60.05	5.01
12	RML	Cent. D	SCLC	23.92	4.22
13	LLL	Cent. D	SCC	9.66	3.01
14	RUL	Cent. D	SCC	47.62	5.11
15	RML	Cent. D	SCC	576.77	10.3
16	RML	Cent. D	SCC	127.22	6.21
17	LUL	Peri. D	SCC	65.89	5.98
18	RLL	Peri. D	SCC	117.7	5.8
19	RUL	Peri. D	Adeno.	9.09	2.7
20	RUL	Peri. D	Adeno.	18.13	3.8
21	LUL	Peri. D	Adeno.	28.26	4.3
22	RUL	Peri. D	Adeno.	13.62	2.87
23	LLL	Peri. D	SCC	51.64	4.9
24	LUL	Peri. D	SCC	7.72	2.7
25	LLL	Peri. D	Adeno.	154.87	6.77
26	RUL	Peri. D	LCC	39.5	4.52
27	RUL	Peri. D	Adeno.	17.07	3.81
28	LLL	Peri. D	SCLC	3.62	2.4
29	RUL	Peri. D	Adeno.	13.77	3.22
30	RUL	Peri. D	SCC	1.78	1.5
31	RLL	Peri. D	SCC	34.77	4.22
32	RUL	Peri. D	SCC	31.88	3.9
33	RLL	Peri. D	SCC	2.16	1.6

Abbreviations: Tum. ID., tumor ID number; Vol., Tumor Volume; Dmax, Maximum diameter; Peri. D, peripheral disease; Cent. D, central disease; LUL, left upper lobe; LLL, left lower lobe; RUL, right upper lobe; RML, right middle lobe; RLL, right lower lobe; SCC, squamous cell carcinoma; Adeno., Adenocarcinoma; LCC, Large-cell carcinoma; SCLC, small cell lung cancer

Results

The image quality of the CBCT was not always sufficient to verify the tumor position in all the cases, partly because intrafractional lung motion blurred the tumors. Therefore, to exclude the impact of intrafractional lung motion for easy recognition the small markers from CBCT images, we only selected patients with breathing motion of ≤ 5 mm; as stated above, the tumor motion was evaluated using a Varian Ximatron Simulator before the CT simulation. Thus, 29 patients with 33 tumors including 16 central and 17 peripheral tumors were analyzed retrospectively. The clinical characteristics of these patients are summarized in Table 1. The tumor volumes

Table 2. Descriptive Statistics of the Surrogates for the Central Lung Tumors (cm)

Surrogate	Mean	SD	95% Confidence interval of means Lower bound	Upper bound	Minimum	Maximum
Vertebrae	0.47	0.27	0.33	0.62	0.25	1.32
Carina	0.39	0.22	0.28	0.51	0.15	0.88
Bronchi	0.32	0.15	0.24	0.4	0.1	0.64
Tumor	0.28	0.13	0.31	0.41	0.05	1.32

Table 3. Descriptive Statistics of the Surrogates for Peripheral Lung Tumors (cm)

Surrogate	Mean	SD	95% Confidence interval of means Lower bound	Upper bound	Minimum	Maximum
Tumor	0.3	0.19	0.2	0.4	0.06	0.71
Vertebrae	0.46	0.39	0.26	0.66	0.1	1.5
Carina	0.64	0.45	0.41	0.87	0.11	1.82
Rib	0.44	0.28	0.3	0.58	0.09	1.05

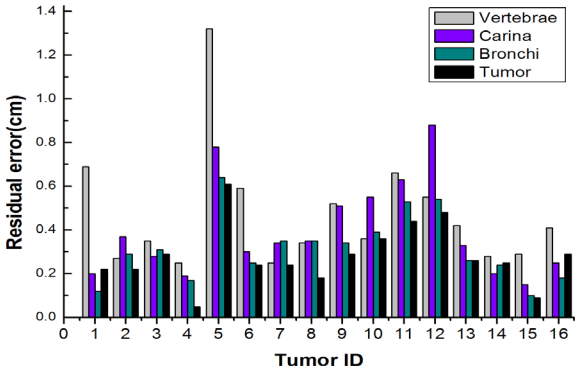

Figure 3. Residual Errors (REs) After Manual Registration with Different Surrogates for the Central Lung Tumors

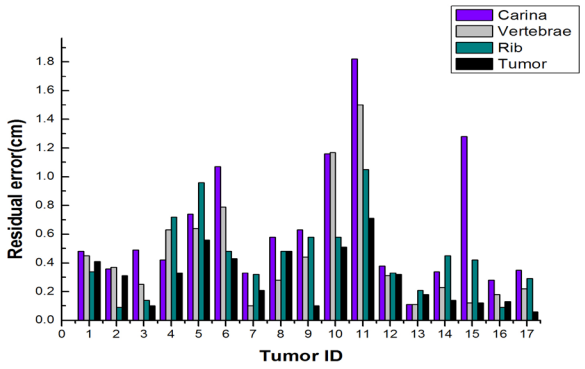

Figure 4. REs After Manual Registration with Different Surrogates for the Peripheral Lung Tumors

of these patients ranged from 1.78 to 576.77 cm^3 with a median of 25.15 cm^3; the maximum diameters of these tumors ranged from 1.50 to 10.30 cm with a median of 4.22 cm.

Surrogates of central lung cancer

The REs after manual registration with different surrogates for 16 central lung tumors are shown in Figure 3. The descriptive statistics of "tumor" and the other 3 surrogates are given in Table 2. The REs (mean ± SD) increased in an ascending order: "tumor" (0.28 ± 0.13 cm), "bronchi" (0.32 ± 0.15 cm), "carina" (0.39 ± 0.22 cm), and "vertebrae" (0.47 ± 0.27 cm). There was a significant difference between "tumor" and "vertebrae" ($p = 0.010$); however no statistically significant differences were observed among the other 2 groups ("tumor" vs. "bronchi," $p = 0.631$; "tumor" vs. "carina," $p = 0.119$).

Surrogates of peripheral lung cancer

The REs after manual registration using different surrogates for 17 peripheral lung tumors are shown in Figure 4. The descriptive statistics of "tumor" and the other 3 surrogates are given in Table 3. The REs (mean ± SD) increased in an ascending order: "tumor" (0.30 ± 0.19 cm), "rib" (0.44 ± 0.28 cm), "vertebrae" (0.46 ± 0.39 cm), and "carina" (0.64 ± 0.45 cm). One-way ANOVA showed a significant difference only between "tumor" and "carina" ($p = 0.005$) but not between the other 2 groups ("tumor" vs. "rib," $p = 0.225$; "tumor" vs. "vertebrae," $p = 0.180$).

Discussion

During the course of online image guidance, it is not always easy to manually match the corresponding tumors of CBCT and planning CT images directly. Therefore, it is necessary to screen the surrogate of lung tumors for online image guidance. In this study, we reported the initial results of the anatomic accuracy of several candidate surrogates for image-guided lung radiotherapy according to the REs after manual matching. Assuming that the optimal surrogates of central and peripheral intrapulmonary tumors are different, we evaluated the geometric accuracy of the "large bronchi," "tracheal carina," and "thoracic vertebrae" as candidate surrogates of central lung lesions and "rib," "thoracic vertebrae," and "tracheal carina" as candidate surrogates of peripheral lung tumors for IGRT. Our results showed that "thoracic vertebrae" and "tracheal carina" are not suitable surrogates for central lesions and peripheral lung disease, respectively. Therefore, when it is difficult to directly match tumors between online volumetric images and planning CT images manually, we suggest that soft-tissue matching combining "large bronchi" and "tracheal carina" should be chosen as a registration template for central lung diseases; meanwhile, bone tissue matching combining "rib" and "thoracic vertebrae" would be a better choice for peripheral lung cancer. In some treatment centers where online 2D imaging devices such as EPIDs are the main instruments for image guidance, it would be better to use corresponding anatomic landmarks instead of a blurred tumor itself as the surrogate for image guidance according to the location of lung cancer.

One potential drawback of using daily online matching is the extra time required for treatment sessions, especially when the comparison is visual or manual. Therefore, implementing training for online registration techniques would reduce the amount of time required for performing manual matching (Fox et al., 2006; Perkins et al., 2006; Rodríguez and Cordón, 2009). At present, manual registration does not exceed 4 min in comparison to the 30 s needed for computer-automated registration of the online CBCT and reference CT images at our treatment center, which is similar to that reported by Fox et al (Fox et al., 2006). In a study at the Princess Margaret Hospital,

Canada (Higgins et al., 2009) the image-guided process took an average of 4 min for manual tumor matching, which was deemed unsatisfactory. In fact, a protocol including CBCT imaging, manual matching, and setup correction adds approximately 4–6 min to the total treatment time, which ranges from 20–40 min depending on the dose fractionation and number of beams. So, it is acceptable for the amount of time added to either manual or automatic registration of planning and verification CT. In this study, all the manual matching processes of image-guided treatments were successfully completed for every patient.

Higgins et al. (2009) also evaluated the reproducibility of volumetric lung image guidance according to the intraclass correlations, which were calculated using absolute couch shift values after matching (i.e., manual vertebrae, manual carina, manual tumor); they recommend that the vertebrae and carina are the better surrogates of the target than manual tumor matching because of the shorter time required for manual tumor matching as well as the greater reproducibility of manual matching based on "vertebrae" or "carina" as compared to manual tumor matching. However, the matching time, reproducibility, and accuracy of manual matching are usually related to the shape and volume of the target. If the tumor is small enough, the matching time will be short and the reproducibility and accuracy of manual matching would be perfect. However, if the tumor is large and irregularly shaped, adjacent image slices would obviously differ, and it will be easy to find the corresponding slices of planning and online CT. Consequently, a perfect registration can be reached quickly; meanwhile, the reproducibility would also be good. If the tumor is round or oval and is large, the image slices adjacent to each other would be so similar that manual slice-to-slice matching would be difficult; consequently, the reproducibility and accuracy would be poor. Therefore, it is not suitable to screen potential surrogates for manual matching merely according to the matching time and reproducibility.

With a CBCT image acquisition time of approximately 1.0 min, moving organs are blurred in direction of the movement. Therefore, CBCT images acquired prior to treatment not only provide information about the position of the tumor but also the range and pattern of tumor motion. Because the "rotation time" of the simulation CT gantry at our clinic is 1.0 s, the planning CT images involve partial information regarding tumor motion. There are systematic errors during online matching of the CBCT to the planning CT, therefore, we only selected patients with breathing motion of ≤ 5 mm to exclude the impact of intrafractional lung motion for easy recognition of small markers from CBCT images. Even though our study presents a new method for evaluating the accuracy of different anatomic landmarks as surrogates of irradiation targets for volumetric image guidance, it would be better to employ a slow CT scan, average CT from planning 4DCT to match the CBCT results. Therefore, we can match the actual and planned tumors according to a homogenous shape.

Acknowledgements

This work was supported in part by 30970861 from National Nature Science Foundation of China and 2011GSF11824 from the Science and Technology Project of Shandong Province, China. The authors would like to thank the reviewers for their insightful suggestions, which helped improve the manuscript.

References

Bel A, Keus R, Vijlbrief RE, Lebesque JV (1995). Setup deviations in wedged pair irradiation of parotid gland and tonsillar tumors, measured with an electronic portal imaging device. *Radiother Oncol*, **37**, 153-9.

Bissonnette JP, Purdie TG, Higgins JA, Li W, Bezjak A (2009). Cone-beam computed tomographic image guidance for lung cancer radiation therapy. *Int J Radiat Oncol Biol Phys*, **73**, 927-34.

Boda-Heggemann J, Fleckenstein J, Lohr F, et al (2011). Multiple breath-hold CBCT for online image guided radiotherapy of lung tumors: simulation with a dynamic phantom and first patient data. *Radiother Oncol*, **98**, 309-16.

Chen AM, Farwell DG, Luu Q, et al (2011). Evaluation of the planning target volume in the treatment of head and neck cancer with intensity-modulated radiotherapy: what is the appropriate expansion margin in the setting of daily image guidance? *Int J Radiat Oncol Biol Phys*, **81**, 943-9.

de Boer HC, van Sornsen de Koste JR, et al (2001). Electronic portal image assisted reduction of systematic set-up errors in head and neck irradiation. *Radiother Oncol*, **61**, 299-308.

Dirkx ML, de Boer JC, Heijmen BJ (2006). Improvement of radiotherapy treatment delivery accuracy using an electronic portal imaging device. *Radiat Prot Dosimetry*, **121**, 70-9.

Fox TH, Elder ES, Crocker IR, et al (2006). Clinical implementation and efficiency of kilovoltage image-guided radiation therapy. *J Am Coll Radiol*, **3**, 38-44.

Grills IS, Hugo G, Kestin LL, et al (2008). Image-guided radiotherapy via daily online cone-beam CT substantially reduces margin requirements for stereotactic lung radiotherapy. *Int J Radiat Oncol Biol Phys*, **70**, 1045-56.

Guckenberger M, Meyer J, Wilbert J, et al (2006). Cone-beam CT based image-guidance for extracranial stereotactic radiotherapy of intrapulmonary tumors. *Acta Oncol*, **45**, 897-906.

Guckenberger M, Meyer J, Wilbert J, et al (2007). Intra-fractional uncertainties in cone-beam CT based image-guided radiotherapy (IGRT) of pulmonary tumors. *Radiother Oncol*, **83**, 57-64.

Herman MG, Balter JM, Jaffray DA, et al (2001). Clinical use of electronic portal imaging: report of AAPM Radiation Therapy Committee Task Group 58. *Med Phys*, **28**, 712-37.

Higgins J, Bezjak A, Franks K, et al (2009). Comparison of spine, carina, and tumor as registration landmarks for volumetric image-guided lung radiotherapy. *Int J Radiat Oncol Biol Phys*, **73**, 1404-13.

Higgins J, Bezjak A, Hope A, et al (2011). Effect of Image-Guidance Frequency on Geometric Accuracy and Setup Margins in Radiotherapy for Locally Advanced Lung Cancer. *Int J Radiat Oncol Biol Phys*, **80**, 1330-7.

Perkins CL, Fox T, Elder E, et al (2006). Image-guided radiation therapy (IGRT) in gastrointestinal tumors. *Jop*, **7**, 372-81.

Purdie TG, Bissonnette JP, Franks K, et al (2007). Cone-beam computed tomography for on-line image guidance of lung stereotactic radiotherapy: localization, verification, and

intrafraction tumor position. *Int J Radiat Oncol Biol Phys*, **68**, 243-52.

Rodríguez Cordón M, Ferrer Albiach C (2009). Theoretical aspects of implementation of kilovoltage cone-beam CT onboard linear accelerator for image-guided radiotherapy. *Clin Transl Oncol*, **11**, 511-7.

Song S, Choi E, Lee J, et al (2007). Image guided radiation therapy using cone-beam computed tomography in stereotactic radiosurgery for lung tumor. *Int J Radiat Oncol Biol Phys*, **69**, S482.

Thilmann C, Nill S, Tucking T, et al (2006). Correction of patient positioning errors based on in-line cone beam CTs: clinical implementation and first experiences. *Radiation oncology (London, England)*, **1**, 16.

Wang YY, Fu XL, Yang HJ, et al(2007). Residual error of the online kilovoltage cone-beam ct guided radiotherapy evaluated in phantom and thoracic cancer patients. *Int J Radiat Oncol Biol Phys*, **69**, S499-500.

Yeung AR, Li JG, Shi W, et al (2009). Tumor localization using cone-beam CT reduces setup margins in conventionally fractionated radiotherapy for lung tumors. *Int J Radiat Oncol Biol Phys*, **74**, 1100-7.